Monte Carlo simulation of SiO_2 nanoparticle-coated polymer optical fiber humidity sensor by ray tracing

Milan S. KOVACEVIC[1], Marko M. MILOSEVIC[1],
Ljubica KUZMANOVIC[1], Alexandar DJORDJEVICH[2]

[1]Faculty of Science University of Kragujevac, Serbia

[2]City University of Hong Kong, Hong Kong

A fiber optic device sensitive to humidity is detailed and modelled by ray tracing based on Monte Carlo simulation. The device is intended primarily for monitoring humidity in the microenvironment of wounds without removing the wound dressing and thus disturbing the wound-healing process. To produce the sensor, cladding is removed from a segment of its polymer-fiber and mesoporous SiO_2 nanoparticles are deposited in the exposed zone. This introduces an additional light-transmission loss. The extent of such loss is related to the relative humidity of the environment. Such a relationship, embodying the essence of the sensor's modulation principle, is examined in this paper by ray tracing based on Monte Carlo simulation. The sensor is explained in detail and its performance is characterised.

Keywords: optical fiber, humidity, ray propagation, ray tracing.

1. Introduction

Measurement of humidity is valued highly not only in meteorological forecasting, air conditioning and farming but also in the manufacturing of numerous products such as pharmaceuticals and materials engineering. It has also been of interest in fiber-optics as the radiation loss may depend on the relative humidity. A considerable body of research has been devoted to fiber-optic (FO)-based techniques for humidity sensing. An overview of fiber-optic-based methods for humidity sensing is given in [1]. They are cross compared to non-FO methods in [2]. Optical fiber humidity sensors are further elaborated in [3, 4], covering both extrinsic and intrinsic sensor types. Based on their working principle, FO sensors have been described that operate on the basis of absorption [5–9], interference in general [10–12], fiber Bragg grating [13–16], and electromagnetic resonance [17–19].

Polymer optical fibers (POFs) have much potential in sensing applications. Compared to their glass counterparts, they are less costly and easier to handle. POF humidity sensor (POFHS) has been proposed [20]. Its signal is modulated by the evanescent

wave (EW) interreacting with the hydrophilic film whose refractive index changes in the presence of water molecules that tend to attach to it.

In the earlier publications various accurate methods of multimode fibers modal analysis is exploited. For example, the method that relies on the solving power flow equations was described in [21–24]. The solution gives the angular properties of the beam that originates from a prescribed source distribution and propagates down the multimode fiber. In this paper there is a report that applied the ray tracing model to simulate of POF humidity sensor characteristics and compare the experimental result that has been reported in [20].

2. Polymer optical fiber humidity sensor – an overview

An intensity-modulated optical-fiber humidity sensor measures light intensity that varies due to the evanescent wave interreacting with the hydrophilic film. Commercial fiber ESKA SK-10 (by Mitsubishi Rayon Co., Ltd.) was used to build the sensor. This multimode (step index) polymer fiber has the polymethyl-methacrylate resin core with the diameter of 240 µm. Its index of refraction is 1.49 and numerical aperture 0.5. Its core is cladded in a 5 µm fluorinated polymer. The optical fiber of the humidity sensor is specially sensitized by precision machining into the cladding of a selected fiber segment. This removed the cladding and a portion of the fiber core along a selected fiber segment as illustrated in Fig. 1.

The length and depth of the sensing zone affect the sensitivity. Once the cladding and a part of the core are removed, a film sensitive to humidity is deposited using the LbL method. It consists of SiO_2 mesoporous nanoparticles (SNOWTEX 20L, 40–50 nm diameter, Nissan Chemical, Japan). They were deposited with poly(allylamine hydrochloride) (PAH) to form a PAH/SiO_2 hydrophilic material. This combination provided a higher sensitivity to humidity [25]. The deposition of the PAH/SiO_2 layers was in three stages [26]. The resulting cut-out introduced light transmission loss that is related to relative humidity. Such a relationship, embodying the essence of the sensor's modulation principle, is examined in this paper by ray tracing based on Monte Carlo simulation.
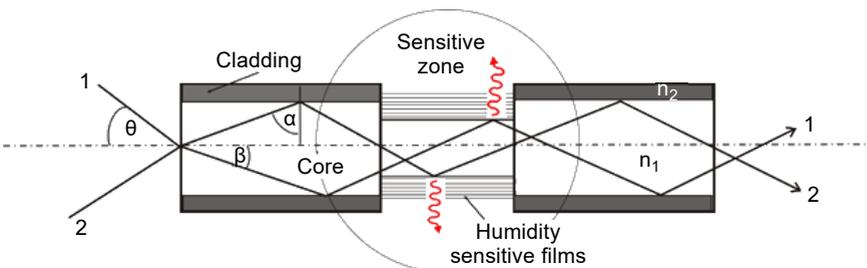
Fig. 1. Ray representation in light propagation along the sensitized FOHS.

3. Three-dimensional ray-trace modelling of POFHS

Using Monte Carlo simulation, the basic idea is to trace rays propagating along the fiber that has the sensitised zone. Rays radiated through the sensitive zone represent a modulation loss induced by the sensor – for the particular level of relative humidity taken as a reference. At different humidity, the ratio of this light loss to that in the sensitive zone at reference humidity level is then calculated (under equal other conditions). The magnitude of this relative loss characterises the device sensitivity for the particular set of the sensitive zone's features, chiefly the zone length, depth and the number/type of deposited layers. Because it would be difficult to optimise these multiple sensor-features experimentally, a computer optimisation is performed by ray tracing.

Monte Carlo simulation is used to generate random directions for many input rays (more than 10^6). Each such launch is traced as it propagates along the POF until either contributing to a radiation loss or reaching the output fiber end. To represent light originating from a point-source at the center of the input fiber-end, two angles are used to describe the launch directions with respect to the fiber axis: θ and φ. The latter angle is sampled uniformly in the range 0–2π by the standard random number γ_1 distributed uniformly between 0 and 1:

$$\varphi = 2\pi\gamma_1 \tag{1}$$

Angle θ is sampled as a Gaussian distribution with standard deviation σ:

$$f(\theta) = \frac{1}{\sqrt{2\pi}\,\sigma}\exp\left[-\frac{(\theta-\theta_0)^2}{2\sigma^2}\right] \tag{2}$$

The mean angle θ_0 in (2) is from the function GASDEV (Gaussian deviates) that is a part of a program library [27]. The overall number of rays launched is a fixed parameter.

Together, Equations (1) and (2) model the input distribution in three dimensions. Every ray direction thus generated is from an isotropic point-source eradiating the input fiber-end as a convex spherical surface distance of H from it, in a medium with the refractive index n_0. While a different launch arrangement would be possible, mode coupling is strong in POFs causing all input distributions to converge rapidly (to what is called equilibrium mode distribution consistent with the said two equations). Further ray trajectories with distance from input fiber-end are traced by the method described previously [28, 29].

4. Results

The important part of the simulation is to trace rays as they propagate along the sensitized zone of the multimode POF (ESKA SK-10 multimode POF, Mitsubishi Rayon Co. Ltd. with the core diameter of 240 μm, 1.49 core refractive index and 5 μm thick

fluorinated polymer cladding; NA = 0.5). A 125 mW point source was situated distance 100 μm from the input fiber end. The axial location at the start of the zone is specified as an input parameter $z = z_1$ along the fiber axis. The zone is rough, and the depth of the zone is fixed. Sensing region's lengths of 5, 10, 20 and 30 mm were modelled for the core diameter reduced to 190 μm. The condition for total reflection was examined for each ray at every reflection. The program recorded the outcomes. If a ray reached the sensitized zone, its transmission loss was also recorded. To compare the interaction of the evanescent wave with different lengths of the sensitive zone, the transmittance at wavelength of 611 nm was calculated as a function of length of the unclad section of the POF. The transmittance is simply calculated as the ratio $(P_{out}/P_{in}) \times 100\%$ where P_{out} is total optical power at the end face of the fiber, and P_{in} is the total initial power at the fiber origin.

For a 25 μm deep zone, the transmittance as a function of the zone length is given in Fig. 2. It is observed that with an increased length of the zone, less light reaches the end of the fiber. In other words, the longer the unclad region, the more of the light escapes from the fiber core. A decreasing logarithmic function for transmittance *vs.* length of the zone was fitted to represent these results.

Figure 3 shows transmittance as a function of the number of PAH/SiO$_2$ layers deposited. The hydrophilic mesoporous films are deposited layer by layer on the unclad central region of the POF. The light intensity change in the interaction of the evanescent wave with the hydrophilic film is calculated as well.

Light traveling through a step-index POF is guided within the core as a result of the total internal reflection if the critical angle criterium is fulfilled. If the light riches the region with hydrophilic mesoporous films, at each point it generates a standing wave that extends beyond the core of the fiber and penetrates the layer region of the FOHS. A PAH/SiO$_2$ layer is approximately 45 nm thick so after 7 layers the deposited film thickness is close to 360 nm. In the computer simulation, the exponential amplitude
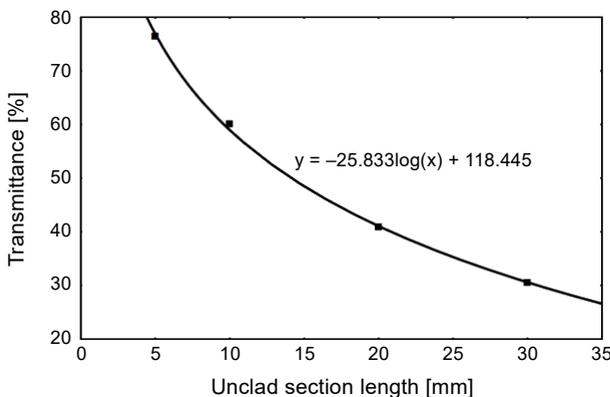
Fig. 2. Transmittance *vs.* the length of the unclad section of the POF.
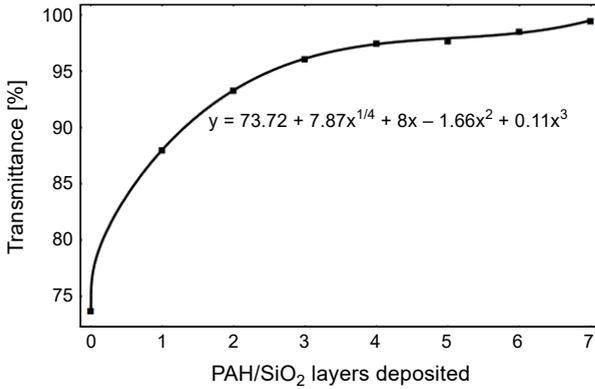
Fig. 3. Transmittance at 611 nm *vs.* the number of layers deposited.

decay of the evanescent field with distance from the core is considered when calculating transmittance. Results have been fitted with the polynomial function of the third order. This method allows the optical fiber to be used as a sensor where the field generated at the interface with the target surrounding the fiber, thus giving information as a result of optical absorption.

Figure 4 shows the calculations with POFHS coated with five and seven PAH/SiO$_2$ layers. Calculations are for the wavelength of 611 nm for both sensors (190 μm core diameter and 30 mm length of the sensitive region).

Relative humidity represents the ratio of the amount of water vapour present in the atmosphere to the maximum amount the atmosphere can hold and is often expressed as a percentage. From the graphical interpretation of the results in Fig. 4, it can be observed that the POFHS sensitivity increases as the number of layers increases.
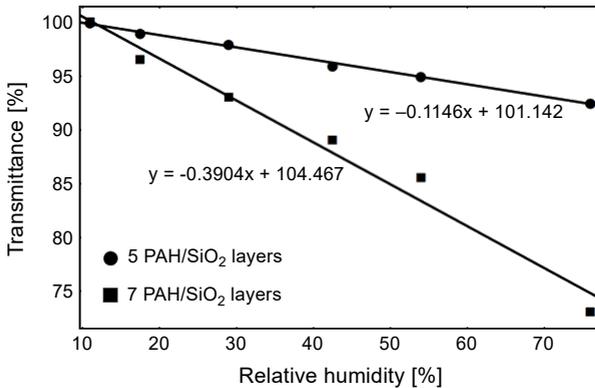
Fig. 4. Transmittance *vs.* relative humidity. The curves of a POFHS coated with five and seven PAH/SiO$_2$ layers. Calculations were for the wavelength of 611 nm, for the core diameter of 190 μm and for 30 mm long sensitive region.

5. Conclusion

Low cost, ease of termination/coupling and relatively high resistance to fracture of plastic optical fibers relative to those of their counterparts made of glass have long been attracting a considerable amount of research interest. Furthermore, plastic fibers' use as sensors often requires not much more than basic (inexpensive) devices such as light emitting and photodiodes. In this paper, three-dimensional analysis of light propagation through the optical fiber humidity sensor is reported. The sensor characteristics are simulated in order to analyse and compare the experimental results. All major cases that may appear when light interacts with the device's sensitive zone have been considered. This simulation includes different lengths of the sensitive zone of the POF. In the computer experiment, the penetration depth of the evanescent wave and its interaction with the hydrophilic film is related to the light loss that reaches the sensitized region. The refractive index of PAH/SiO$_2$ layers was altered by, and the fiber transmittance was calculated as a function of, relative humidity. From the graphical interpretation of our results in Figure 4, the calibration curve for the humidity sensor is determined as

transmittance = –0.11 relative humidity + 101.142

transmittance = –0.390 relative humidity + 104.467

for sensors with five and seven PAH/SiO$_2$ layers, respectively. These results are in good agreement with previous experimental results [20].

References

[1] Yeo T.L., Sun T., Grattan K.T.V., *Fibre-optic sensor technologies for humidity and moisture measurement*, Sensors and Actuators A: Physical **144**(2), 2008, pp. 280–295, DOI: 10.1016/j.sna.2008.01.017.

[2] Wiederhold P.R., *Water Vapor Measurements: Methods and Instrumentation*, CRC Press, 1997, DOI: 10.1201/9781466551978.

[3] Grattan K.T.V., Sun T., *Fibre optic sensor technology: an overview*, Sensors and Actuators A: Physical **82**(1–3), 2000, pp. 40–61, DOI: 10.1016/S0924-4247(99)00368-4.

[4] Grattan L.S., Meggitt B.T. [Eds.], *Optical Fiber Sensor Technology, Volume 4: Chemical and Environmental Sensing*, Springer Netherlands, 1999, DOI: 10.1007/978-94-017-2484-5.

[5] Aneesh R., Khijwania S.K., *Zinc oxide nanoparticle based optical fiber humidity sensor having linear response throughout a large dynamic range*, Applied Optics **50**(27), 2011, pp. 5310–5314, DOI: 10.1364/AO.50.005310.

[6] Luo Y., Chen C., Xia K., Peng S., Guan H., Tang J., Lu H., Yu J., Zhang J., Xiao Y., Chen Z., *Tungsten disulfide (WS$_2$) based all-fiber-optic humidity sensor*, Optics Express **24**(8), 2016, pp. 8956–8966, DOI: 10.1364/OE.24.008956.

[7] Zhao Z. Duan Y., *A low cost fiber-optic humidity sensor based on silica sol–gel film*, Sensors and Actuators B: Chemical **160**(1), 2011, pp. 1340–1345, DOI: 10.1016/j.snb.2011.09.072.

[8] Otsuki S., Adachi K., *Humidity dependence of visible absorption spectrum of gelatine films containing cobalt chloride*, Journal of Applied Polymer Science **48**(9), 1993, pp. 1557–1564, DOI: 10.1002/app.1993.070480907.

[9] Tao S., Winstead C.B., Jindal R., Singh J.P., *Optical-fiber sensor using tailored porous sol–gel fiber core*, IEEE Sensors Journal **4**(3), 2004, pp. 322–328, DOI: 10.1109/JSEN.2004.827274.

[10] Wu Q., Semenova Y., Mathew J., Wang P., Farrell G., *Humidity sensor based on a single-mode hetero-core fiber structure*, Optics Letters **36**(10), 2011, pp. 1752–1754, DOI: 10.1364/OL.36.001752.

[11] Villatoro J., Finazzi V., Badenes G., Pruneri V., *Highly sensitive sensors based on photonic crystal fiber modal interferometers*, Journal of Sensors, Vol. 2009, 2009, article 747803, DOI: 10.1155/2009/747803.

[12] Lopez-Torres D., Elosua C., Villatoro J., Zubia J., Rothhardt M., Schuster K., Arregui F.J., *Photonic crystal fiber interferometer coated with a PAH/PAA nanolayer as humidity sensor*, Sensors and Actuators B: Chemical **242**, 2017, pp. 1065–1072, DOI: 10.1016/j.snb.2016.09.144.

[13] Othonos A., *Bragg gratings in optical fibers: fundamentals and applications*, [In] *Optical Fiber Sensor Technology*, [Eds.] Grattan K.T.V., Meggitt B.T., Springer, Boston, MA, 2000, DOI: 10.1007/978-1-4757-6079-8_2.

[14] Rao Y.J., *Recent progress in applications of in-fibre Bragg grating sensors*, Optics and Lasers in Engineering **31**(4), 1999, pp. 297–324, DOI: 10.1016/S0143-8166(99)00025-1.

[15] James S.W., Tatam R.P., *Optical fibre long-period grating sensors: characteristics and application*, Measurement Science and Technology **14**(5), 2003, pp. R49–R61, DOI: 10.1088/0957-0233/14/5/201.

[16] Sutapun B., Tabib-Azar M., Kazemi A., *Pd-coated elastooptic fiber optic Bragg grating sensors for multiplexed hydrogen sensing*, Sensors and Actuators B: Chemical **60**(1), 1999, pp. 27–34, DOI: 10.1016/S0925-4005(99)00240-3.

[17] Hernáez M., Zamarreño C.R., Matías I.R., Arregui F.J., *Optical fiber humidity sensor based on surface plasmon resonance in the infra-red region*, Journal of Physics: Conference Series **178**, 2009, article 012019, DOI: 10.1088/1742-6596/178/1/012019.

[18] Hernáez M., Del Villar I., Zamarreño C.R., Arregui F.J., Matias I.R., *Optical fiber refractometers based on lossy mode resonances supported by TiO$_2$ coatings*, Applied Optics **49**(20), 2010, pp. 3980–3985, DOI: 10.1364/AO.49.003980.

[19] Ascorbe J., Corres J.M., Matias I.R., Arregui F.J., *High sensitivity humidity sensor based on cladding-etched optical fiber and lossy mode resonances*, Sensors and Actuators B: Chemical **233**, 2016, pp. 7–16, DOI: 10.1016/j.snb.2016.04.045.

[20] Gomez D., Morgan S.P., Hayes-Gill B.R., Goncalves Correia R., Korposh S., *Polymeric optical fibre sensor coated by SiO$_2$ nanoparticles for humidity sensing in the skin microenvironment*, Sensors and Actuators B: Chemical **254**, 2018, pp. 887–895, DOI: 10.1016/j.snb.2017.07.191.

[21] Drljaca B., Savovic S., Djordjevich A., *Calculation of the frequency response and bandwidth in step-index plastic optical fibres using the time-dependent power flow equation*, Physica Scripta **2012**(T149), 2012, article 014028, DOI: 10.1088/0031-8949/2012/T149/014028.

[22] Savovic S., Djordjevich A., Simovic A., Drljaca B., *Influence of mode coupling on three, four and five spatially multiplexed channels in multimode step-index plastic optical fibers*, Optics and Laser Technology **106**, 2018, pp. 18–21, DOI: 10.1016/j.optlastec.2018.03.015.

[23] Savovic S., Drljaca B., Djordjevich A., *Influence of launch-beam distribution on bandwidth in step-index plastic optical fibers*, Applied Optics **52**(6), 2013, pp. 1117–1121, DOI: 10.1364/AO.52.001117.

[24] Mateo J., Losada M.A., Zubia J., *Frequency response in step index plastic optical fibers obtained from the generalized power flow equation*, Optics Express **17**(4), 2009, pp. 2850–2860, DOI: 10.1364/OE.17.002850.

[25] Viegas D., Goicoechea J., Santos J.L., Moita Araujo F., Ferreira L.A., Arregui F.J., Matias I.R., *Sensitivity improvement of a humidity sensor based on silica nanospheres on a long-perios fiber grating*, Sensors **9**(1), 2009, pp. 519–527, DOI: 10.3390/s90100519.

[26] Korposh S., James S., Tatam R., Lee S.-W., *Fibre-optic chemical sensor approaches based on nanoassembled thin films: a challenge to future sensor technology*, [In] *Current Developments in Optical Fiber Technology*, [Eds.] Harun S.W., Arof H., IntechOpen, 2013, pp. 237–264, DOI: 10.5772/53399.

[27] Smith I.M., *Programming in Fortran 90: A First Course for Engineers and Scientists*, Wiley, 1995.

[28] Kovacevic M.S., Nikezic D., Djordjevich A., *Modeling of the loss and mode coupling due to an ir-regular core–cladding interface in step-index plastic optical fibers*, Applied Optics **44**(19), 2005, pp. 3898–3903, DOI: 10.1364/AO.44.003898.

[29] Kovačević M., Nikezić D., Djordjevich A., *Monte Carlo simulation of curvature gauges by ray tracing*, Measurement Science and Technology **15**(9), 2004, pp. 1756–1761, DOI: 10.1088/0957-0233/15/9/011.